NiFe 2 O 4 nanoparticles formed in situ in silica matrix by mechanical activation

Z. H. Zhou, J. M. Xue, J. Wang, H. S. O. Chan, T. Yu, and Z. X. Shen

Citation: Journal of Applied Physics **91**, 6015 (2002); doi: 10.1063/1.1462853
View online: http://dx.doi.org/10.1063/1.1462853
View Table of Contents: http://scitation.aip.org/content/aip/journal/jap/91/9?ver=pdfcov
Published by the AIP Publishing

$NiFe_2O_4$ nanoparticles formed *in situ* in silica matrix by mechanical activation

Z. H. Zhou, J. M. Xue, and J. Wang[a)]
Department of Materials Science, Faculty of Science, National University of Singapore, Singapore 119260

H. S. O. Chan
Department of Chemistry, Faculty of Science, National University of Singapore, Singapore 119260

T. Yu and Z. X. Shen
Department of Physics, Faculty of Science, National University of Singapore, Singapore 119260

(Received 5 November 2001; accepted for publication 29 January 2002)

Nanocrystalline nickel ferrite ($NiFe_2O_4$) particles were successfully synthesized *in situ* in an amorphous silica matrix by mechanical activation at room temperature. Phase development in the amorphous precursors, derived via a modified sol–gel synthesis route, with increasing mechanical activation time was studied in detail by employing transmission electron microscopy, x-ray diffraction, and Raman spectroscopy. $NiFe_2O_4$ nanoparticles of 8.05 nm in mean particle size with a standard deviation of 1.24 nm, which were well dispersed in the silica matrix, were realized by 30 h of mechanical activation. The phase formation of nanocrystalline $NiFe_2O_4$ particles involves the nucleation of Fe_3O_4 in amorphous silica at the initial stage of mechanical activation, followed by the growth of nickel ferrite by incorporation of Ni^{2+} caions into Fe_3O_4. Their magnetic anisotropy, surface spin disorder, and cation distribution are investigated by considering both the strain imposed by silica matrix and the buffer effect during mechanical activation. © *2002 American Institute of Physics.* [DOI: 10.1063/1.1462853]

I. INTRODUCTION

Nanophase spinel ferrite particles have attracted considerable attention owing to their technological importance in the application areas, such as microwave devices (microwave absorbers and waveguides in the gigahertz region), high speed digital tape and disk recording, repulsive suspension for use in levitated systems, ferrofluids, catalysis, and magnetic refrigeration systems.[1–4] These applications are critically dependent on the unique physical, structural, and chemical properties of nanosized spinel ferrites. The scientific importance of synthesizing functional nanoparticles lies in the fact that nanosized functional particles exhibit many different anomalous properties. Due to the significant surface-to-volume ratio, anomalous magnetic behaviors, derived from surface spin disorder, have been observed in mechanically activated $NiFe_2O_4$ nanoparticles.[5] Change in cation distribution upon mechanical activation of $NiFe_2O_4$ nanoparticles has also been studied previously using Mössbauer spectroscopy and extended x-ray absorption fine structure.[6] Noninteracting ultrafine $NiFe_2O_4$ particles of single domain exhibit the unusual Hopkinson effect, where magnetization reaches a maximum just below the Curie temperature T_c in the presence of a small external magnetic field.[2,7] The nature of spin structure in these nanoparticles and the physical principles of these anomalous behaviors are not fully understood. Investigations into these unique phenomena and magnetic properties of nanophase ferrite particles remain a scientifically interesting topic.

Both the technological challenge and scientific importance have prompted a search for various synthesis routes of nanocrystalline ferrites, including hydrothermal reaction, electrochemical synthesis, oxidative precipitation, citrate precursor method, and sonochemical decomposition.[2,8–11] However, the tendency of nanocrystallites to aggregate and coarsen at elevated temperatures remains a critical obstacle for most of these synthesis techniques in realizing and assembling the required nanoparticles. Mechanical activation is a synthesis technique for nanophase materials. $NiFe_2O_4$, $ZnFe_2O_4$, $MnFe_2O_4$, and $CoFe_2O_4$ have been successfully synthesized by mechanical activation from oxide compsitions.[12–15] However, the mechanically activated ferrite phases often exhibit poor particle and crystallite characteristics, such as a wide crystallite size distribution, irregular crystallite morphology, and a degree of unwanted crystallite aggregation, although they show well-established nanocrystalline structures.

To avoid the unwanted crystallite coarsening and particle aggregation, attempts have been made to synthesize nanoparticles dispersed in a suitable matrix, for example, in an ion-exchange resin, polymeric wax, polymer films, and silica glass.[16–21] Almost all the wet-chemistry synthesis routes involve a calcination step at elevated temperatures in order to convert the precursor into a designed nanocrystalline phase. In this article, we investigate the feasibility of synthesizing nanocrystallite $NiFe_2O_4$ particles in an amorphous silica matrix formed *in situ* by mechanical activation at room temperature, where the nucleation and growth of nanophase $NiFe_2O_4$ are triggered by mechanical activation, instead of by thermal activation. The silica matrix is considered not

a)Author to whom correspondence should be addressed; electronic mail: maswangj@nus.edu.sg

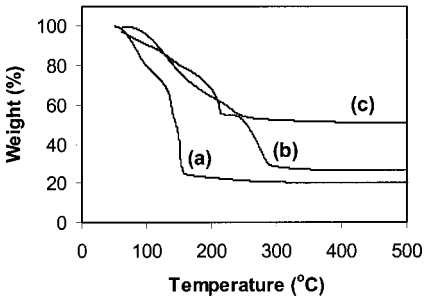

FIG. 1. TGA curves for: (a) $Fe(NO_3)_3 \cdot 9H_2O$, (b) $Ni(NO_3)_2 \cdot 6H_2O$, and (c) mixed $Fe(NO_3)_3 \cdot 9H_2O$ and $Ni(NO_3)_2 \cdot 6H_2O$ in alcogels.

only to serve as spatial nucleation sites for $NiFe_2O_4$, but also to confine the coarsening of nanoparticles as well as to minimize the degree of crystallite aggregation. The silica network can also act as a buffer to protect the nanoparticles during mechanical activation and hence reduce the surface spin disorder. There can also occur a confinement effect and surface strain on the nanophase particles that enhance their magnetic anisotropy.

II. EXPERIMENT DETAILS

A. Starting materials

The chemicals employed in this work as the starting materials included: iron nitrate ($Fe(NO_3)_3 9H_2O$) of reagent grade with purity $>99\%$ (Fisher Scientific), nickel nitrate ($Ni(NO_3)_2 6H_2O$) of purity $>99\%$ (Fisher Scientific), and tetraethyl orthosilicate (TEOS) of purity $>98\%$ (Aldrich Chemical Company, Inc.).

B. Experimental procedure

The composite precursors of nickel ferrite/silica were prepared via a modified sol–gel synthesis route. TEOS and ethanol (EtOH) were slowly added into an aqueous solution of mixed iron nitrate and nickel nitrate. The amounts of iron and nickel nitrates were controlled for at a Fe/Ni mole ratio of 2, while the $NiFe_2O_4/(NiFe_2O_4+SiO_2)$ weight ratio was controlled by varying the amounts of nitrates and TEOS. The $TEOS/EtOH/H_2O$ molar ratio was fixed at 1:1:5. The mixture initially appeared turbid and then turned transparent with emission of heat upon several minutes of vigorous stirring, indicating that the hydrolysis of TEOS had taken place. Upon completion of hydrolysis, the clear solution was then transferred into a plastic petrie dish with a cover and left for slow gelation, which was accompanied by a volume shrinking. The resulting alcogels were further dried in an oven at 150 and 300 °C for 3 h, respectively, at a slow heating rate of 0.5 °C/min. Use of such a slow heating rate was to facilitate the establishment of a silica network, as any cracks of the gel due to fast heating at this stage could cause the nitrate salts to leach out and decompose into oxides upon the subsequent heat treatment. The choice of 150 and 300 °C was based on the decomposition temperatures of iron and nickel nitrates, as observed in the thermogravimetric analysis (TGA). The TGA curves of the nitrates and alcogels are shown in Fig. 1.

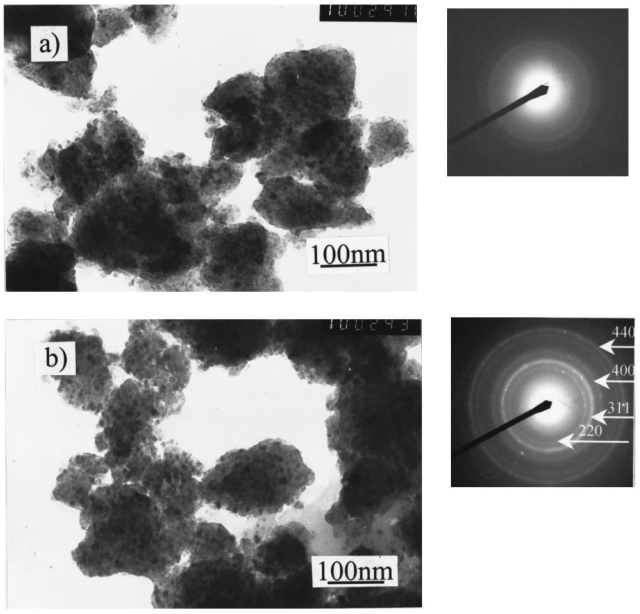

FIG. 2. TEM micrographs and the associated SAD patterns of gel composition subjected to: (a) 5 and (b) 30 h of mechanical activation, respectively.

The *in situ* formation of nickel ferrite nanoparticles in silica matrix was attempted by mechanical activation of the as-dried gel precursor. 3.5 g of the above dried gel were loaded into a cylindrical vial 40 mm in diameter and 40 mm in length together with 15 stainless steel balls 9.24 mm in diameter. The compositions mechanically activated for various time intervals were thoroughly studied for nanocrystalline structure and magnetic behaviors. TGA of iron and nickel nitrates and the alcogels were carried out using a DuPont 2950 thermal analyzer. A powder x-ray diffractometer ($Cu\,K\alpha$, Phillips PW1729 x-ray diffractometer) and Raman spectrometer (Spex 1702/04) were employed to monitor the development of nanocrystallites during the course of mechanical activation. The Raman spectrometer was operated at backscattering geometry with a helium–neon laser operating at 632.8 nm as the excitation source. Transmission electron microscope (TEM) (JEOL-100CX) was used for studies of the particle and crystallite characteristics of nickel ferrite formed *in situ* in the silica matrix. Their magnetic properties were investigated using a vibrating sample magnetometer (Oxford Instruments). A Fourier transform infrared (FT-IR) spectrometer (Bio-rad, FTS 135) was used to investigate the phase evolutions in the nanocomposites.

III. RESULTS AND DISCUSSION

Figures 2(a) and 2(b) are TEM micrographs together with the associated selected area diffraction (SAD) patterns showing the morphologies of nanoparticles formed in the gel compositions subjected to 5 and 30 h of mechanical activation, respectively. A significant amount of nanocrystallites started to nucleate in the amorphous silica matrix upon 5 h of mechanical activation. The poor nanocrystallinity is indicated by the faint halo rings in the associated SAD patterns. The nanocrystallites underwent a steady growth in size with increase in mechanical activation time. Figure 2(b) shows the

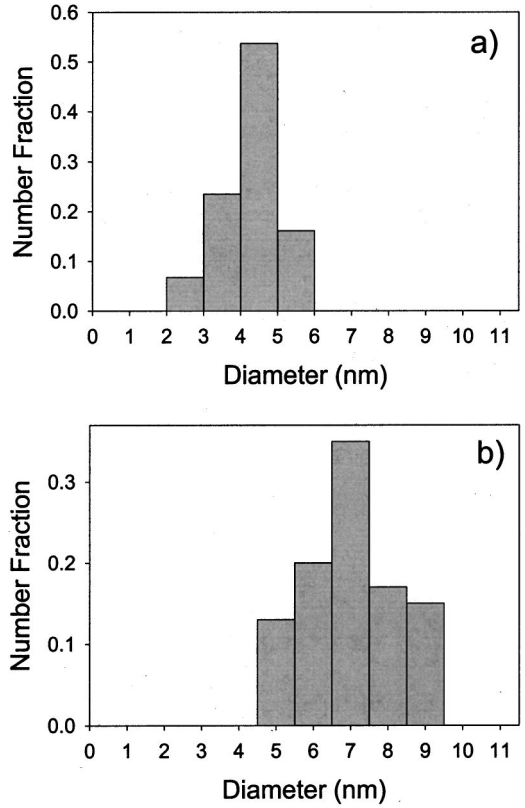

FIG. 3. Size distributions of nanoparticles in the gel compositions subjected to: (a) 5 h and (b) 30 h of mechanical activation.

coarsened nanoparticles that are well dispersed in the silica matrix after mechanical activation for 30 hs. The growth in crystallinity and crystallite size is indicated by the well-defined rings shown in the SAD pattern. Measurements of the diffraction rings confirmed that they correspond to the crystal planes of spinel structure. Figure 3 shows the size distributions of these nanoparticles, as measured from TEM micrographs using an image analyzer, giving a mean size of 8.05 nm and standard deviation of 1.24 nm for the nanoparticles derived from 30 h of mechanical activation, compared to the mean size of 3.74 nm and a standard deviation of 0.78 nm for the material derived from 5 h of mechanical activation. These observations suggest that the formation process of spinel nanocrystallites involve nucleation and subsequent growth in the silica matrix by increasing duration of mechanical activation. Apparently, the aggregation of nanoparticles is minimized by the existence of silica matrix.

The phase formation process in silica matrix triggered by mechanical activation was monitored using x-ray powder diffraction. x-ray diffraction (XRD) traces for the gel compositions mechanically activated for 0, 5, 10, 20, and 30 hs, respectively, are shown in Fig. 4. For the as-dried gel without any mechanical activation, only a very broadened peak over the 2θ range of $20-27°$ is observed, corresponding to the amorphous silica matrix. This indicates that no crystalline phase was formed during the initial drying of the precursor gels at 300 °C. Diffraction peaks started to appear upon 5 h of mechanical activation and their sharpness and intensity were further enhanced with increasing mechanical activation

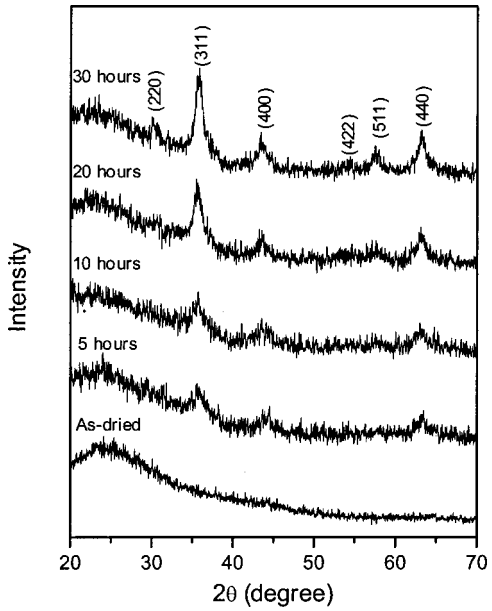

FIG. 4. XRD traces of the as-dried gel containing nickel and iron nitrates in silica upon mechanical activation for different durations.

time. Upon 30 h of mechanical activation, these peaks are well established and they can all be assigned to the spinel structure of either Fe_3O_4 or $NiFe_2O_4$. Intermediate crystalline phases, such as α-Fe_2O_3 or NiO were not detected in the *in situ* formation process of nanocrystalline phase spinel phase.

The above mechanically activated gel compositions were further investigated using Raman spectrometer in order to differentiate $NiFe_2O_4$ from other possible phases, such as Fe_3O_4 and γ-Fe_2O_3, which have similar spinel structures and therefore are similar in XRD patterns. As shown in Fig. 5(a), the Raman spectrum for the gel composition subjected to 5 h of mechanical activation exhibits a weak and broadened peak at $\sim 675\,cm^{-1}$, which can be assigned to Fe_3O_4.[22–24] In contrast, the Raman peaks at 343, 494, 665 (shoulder), and $701\,cm^{-1}$, which are indicative of $NiFe_2O_4$,[25,26] are detected in the spectrum for the gel composition mechanically activated for 30 h [Fig. 5(b)]. Studies of Raman spectroscopy in the high wavenumber region ruled out the existence of γ-Fe_2O_3 in the composition subjected to 30 h of mechanical activation. In conjunction with the results

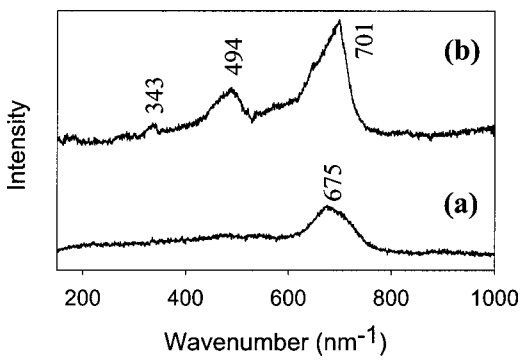

FIG. 5. Raman spectra for the gel compositions subjected to mechanical activation for (a) 5 h and (b) 30 h, respectively.

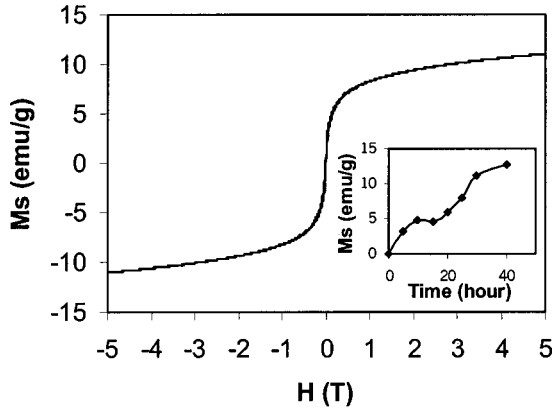

FIG. 6. Magnetization hysteresis loop, measured at room temperature, for gel composition mechanically activated for 30 h. Inset shows the magnetization at 5 T as a function of mechanical activation time.

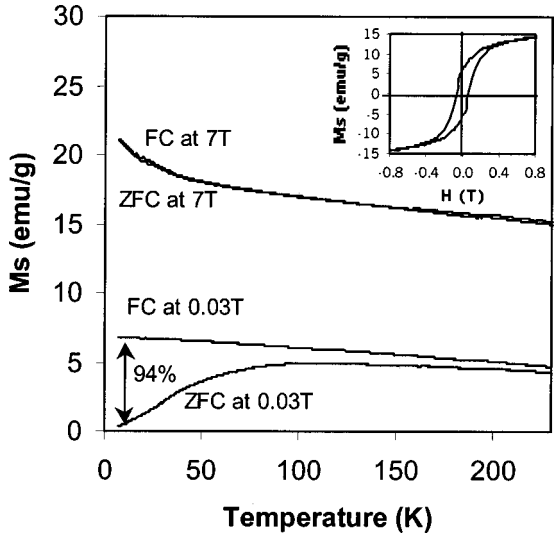

FIG. 7. ZFC and FC magnetization curves measured for the gel composition subjected to 30 h of mechanical activation at an external field of 7 and 0.03 T. Inset is the hysteresis loop in FC state measured at 5 K.

of XRD phase identification, it is suggested that the spinel structure observed at the initial stage of mechanical activation was a result of the nucleation of Fe_3O_4 nanocrystallites in silica. A similar phenomenon was observed by Monte *et al.*[27] and Xue *et al.*,[28] who synthesized γ-Fe_2O_3/SiO_2 nanocomposite by thermal treatment and mechanical activation of TEOS gel containing trivalent Fe ions, respectively. The *in situ* formation of nanocrystalline Fe_3O_4 in silica triggered by mechanical activation was due to the reducing effect of carbonaceous species originated from TEOS.[28] The extension of mechanical activation time gave rise to the formation of nickel ferrite by incorporation of Ni^{2+} ions into Fe_3O_4. The incorporation of Ni^{2+} ions into magnetite particles during crystallization of nickel ferrite was also observed by Regazzoni and Matijevic.[29]

Figure 6 shows the magnetization hysteresis loop for the gel composition mechanically activated for 30 hs. At low field, the loop exhibits zero coercivity and remanence. At high field, magnetization increases almost linearly with the external field and shows a lack of saturation at a field as high as 5 T, which remains evident even at a low temperature of 5 K (shown by the inset in Fig. 7), implying a very large magnetic anisotropy. By considering the confinement effect of silica matrix,[30] this can be accounted for by the surface strain.[31] The magnetization at 5 T as a function of mechanical activation time is presented in the inset of Fig. 6. It is of interest to note that the magnetization increases with activation time up to 10 hs, followed by a slight decrease upon further 5 h of mechanical activation. Further increase in mechanical activation time leads to a steady rise in magnetization, which finally levels off at 30 h of mechanical activation. This is consistent with the phase developments revealed by Raman and XRD studies discussed earlier. The formation of Fe_3O_4 nanocrystallites contributed to the initial increase in magnetization, while the incorporation of Ni^{2+} into Fe_3O_4 led to the occurrence of $NiFe_2O_4$, which exhibits a lower magnetization than that of Fe_3O_4. This responded to the decrease in magnetization observed at 15 h of mechanical activation. With the steady growth of $NiFe_2O_4$ nanoparticles in crystallinity, magnetization recovers and increases with further increase in mechanical activation time.

Previous studies showed anomalous magnetic properties of $NiFe_2O_4$ nanoparticles derived from high-energy ball mill, due to the surface spin disorder.[1,5,6,32] Magnetization measurements at low temperatures were performed in this work to investigate the possible occurrence of surface spin disorder in the nanoparticles of $NiFe_2O_4$ formed *in situ* in the silica matrix. Figure 7 shows the zero-field-cooled (ZFC) and field-cooled (FC) magnetization curves obtained for the gel composition derived from 30 h of mechanical activation at an external field of 7 and 0.03 T, respectively. At the high field of 7 T, the ZFC and FC curves almost completely overlap each other. Separation between ZFC and FC, which was observed for the $NiFe_2O_4$ subjected to high energy ball milling,[5,6] is not shown at the temperature as low as 5 K in this work. At the low field of 0.03 T, a significant difference is observed between ZFC and FC. At 5 K, their difference is $\sim$94%, which is too large to be accounted for by the surface spin canting effect. Rather, it is a result of the superparamagnetic behavior of nanoparticles.[33] For the ferrite particles of 6.5 nm in size, where approximately 26% cations are associated with surfaces, the canted spins can contribute to a $\sim$3% difference between ZFC and FC at 4.2 K.[5] Hysteresis loop shift and high field irreversibility, both of which are associated with the ''freezing'' of disordered surface spins, are not detected in the FC state at 5 K in this work. These experimental results suggest the absence of a large degree of surface spin disorder in the mechanically activated gel compositions. Surface spin disorder in $NiFe_2O_4$ nanoparticles subjected to high energy ball milling is accounted for by the broken exchange bonds between surface spins, which are related to the surface roughness and effects of impurity ions.[1,5,32] The absence of surface spin disorder of $NiFe_2O_4$ nanoparticles in silica synthesized in this work is a result of the matrix buffer that effectively protected the nanoparticles during mechanical activation, minimizing the surface roughness and spin disorder.

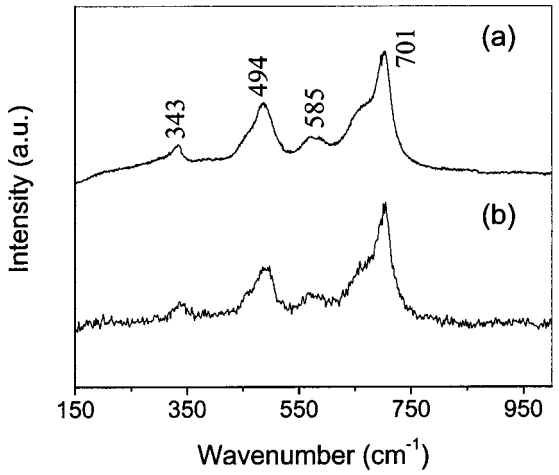

FIG. 8. Raman spectra of (a) the gel composition calcined at 900 °C for 3 h, and (b) gel composition mechanically activated for 30 h and then annealed at 650 °C for 2 h.

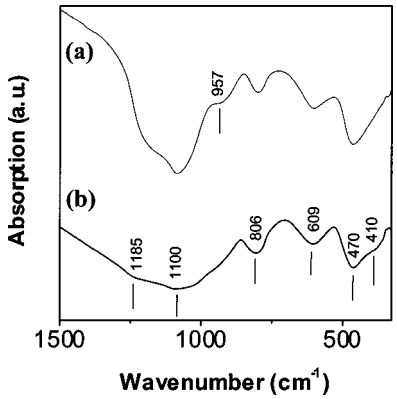

FIG. 9. FT-IR spectra of the gel compositions: (a) mechanically activated for 30 h, and (b) calcined at 900 °C for 3 h, respectively.

To study the cation distribution in $NiFe_2O_4$ nanoparticles formed *in situ* in the silica matrix, samples were synthesized by calcination of the gel composition dried at 300 °C. Figure 8(a) shows Raman spectra for the material calcined at 900 °C for 3 h. All the Raman peaks observed can be assigned to $NiFe_2O_4$. When compared to the Raman spectrum shown in Fig. 5(b) for the $NiFe_2O_4$ nanoparticles derived from mechanical activation, they are much sharpened. However, studies using TEM and XRD phase analysis suggest that the $NiFe_2O_4$ nanoparticles derived from calcination and mechanical activation exhibit similar crystallite sizes. The broadening of Raman peaks observed in Fig. 5(b) is thus due to a high degree of cation disorder, instead of the crystallite size effect.[22,34] It is further noted that the peak at 585 cm^{-1} is dramatically weakened and broadened for the $NiFe_2O_4$ nanoparticles derived from mechanical activation. Since the Raman peaks over the region of 660–720 cm^{-1} reflect the nature of tetrahedra in ferrites, while those in the 460–640 cm^{-1} region reflect the octahedra,[35] this clearly indicates a high degree of disorder in cation distribution in the octahedral sites of the $NiFe_2O_4$ nanoparticles. As also shown in Fig. 8(b), cation reordering can be realized when the gel composition was further annealed at 650 °C for 2 h after mechanical activation, as confirmed by the reappearance of the Raman peak at 585 cm^{-1}. Cation disorder in the $NiFe_2O_4$ particles derived from mechanical activation can be further demonstrated by comparing their FT-IR spectrum [Fig. 9(a)] with that derived from calcination [Fig. 9(b)]. The bands at 470, 806, 957, 1100, and 1185 cm^{-1} correspond to the silica matrix.[36] First, the band at around 957 cm^{-1}, observed for gel composition subjected to mechanical activation, is not detected for the calcined counterpart. It is known to relate to the nonbridging Si–O bonds in silica,[36] suggesting that there occurs a degree of structural defects in the silica network triggered by mechanical activation. The characteristic band of $NiFe_2O_4$ at 609 cm^{-1}, corresponding to the Fe–O bond, appears in both spectra. The other characteristic band of $NiFe_2O_4$ at 410 cm^{-1}, corresponding to the Ni–O bond, was only observed for the $NiFe_2O_4$ derived from calcination at 900 °C. It was not observed for the gel composition derived from mechanical activation. This implies that Ni^{2+} is responsible for the disorder in octahedral sites observed. Disordering of Ni^{2+} has been observed by Chinnasamy *et al.*[6] in their $NiFe_2O_4$ sample subjected to high energy ball milling, where some Ni^{2+} ions were observed to shift from octahedral sites into tetrahedral sites. The disorder of Ni^{2+} cations observed for the $NiFe_2O_4$ particles formed *in situ* in a silica matrix can therefore be attributed to the phase formation process during mechanical activation. The initial mechanical activation led to the nucleation of Fe_3O_4 nanocrystallite, which is followed by the oxidation of Fe^{2+} in the octahedral sites and incorporation of Ni^{2+} into the lattice. Some of the oxidized Fe^{3+} cations remained in the octahedral sites, forcing Ni^{2+} to occupy the tetrahedral sites and giving rise to a disordered cation distribution in $NiFe_2O_4$.

IV. CONCLUSIONS

Nanocrystalline nickel ferrite ($NiFe_2O_4$) particles are triggered to form *in situ* in an amorphous silica matrix by mechanical activation of a sol–gel derived precursor containing nickel and iron nitrates at room temperature. The process involved the nucleation of Fe_3O_4 nanocrystallites in the silica matrix at the initial stage of mechanical activation and the subsequent incorporation of Ni^{2+} into Fe_3O_4 forming $NiFe_2O_4$. Studies of the magnetic properties of the resulting $NiFe_2O_4$ nanoparticles show a large magnetic anisotropy, which is due to the strain imposed by the silica matrix during mechanical activation. The $NiFe_2O_4$ nanoparticles formed *in situ* in silica do not exhibit a large degree of surface spin disorder, as a result of the buffer effect of silica matrix. Disordering of cation distribution, i.e., Ni^{2+} cations occupy the octahedral sites, are shown to occur in these nanocrystalline $NiFe_2O_4$ particles, the reordering of which can be realized by an appropriate thermal treatment at 650 °C.

[1] R. H. Kodama, J. Magn. Magn. Mater. **200**, 359 (1999).
[2] S. Prasad and N. S. Gajbhiye, J. Alloys Compd. **265**, 87 (1998).
[3] M. Gotic, I. Czako-Nagy, S. Popovic, and S. Music, Philos. Mag. Lett. **78**, 13 (1998).
[4] T. Pannaparayil, R. Marande, S. Komameni, and S. G. Sankar, J. Appl. Phys. **64**, 5641 (1998).

[5] R. H. Kodama, A. E. Berkowitz, E. J. Mcniff, and S. Foner, Phys. Rev. Lett. **77**, 394 (1996).
[6] C. N. Chinnasamy, A. Narayanasamy, N. Ponpandian, and K. Chattopadhyay, Phys. Rev. B **63**, 184108 (2001).
[7] J. Loaec, J. Phys. D **26**, 963 (1993).
[8] S. Komarneni, M. C. D'Arrigo, C. Leonelli, G. C. Pellacani, and H. Katsuki, J. Am. Ceram. Soc. **81**, 3041 (1998).
[9] S. D. Sartale and C. D. Lokhande, Indian J. Eng. Mater. Sci. **7**, 404 (2000).
[10] M. Rajendran, A. K. Bhattacharya, D. Das, S. N. Chintalapudi, and C. K. Majumdar, Int. J. Mod. Phys. B **15**, 305 (2001).
[11] K. V. P. M. Shafi, Y. Koltypin, A. Gedanken, R. Prozorov, J. Balogh, J. Lendvai, and I. Felner, J. Phys. Chem. B **101**, 6409 (1997).
[12] V. Sepelak, A. Y. Rogachev, U. Steinike, D. C. Uecker, F. Krumeich, S. Wissmann, and K. D. Becker, Mater. Sci. Forum **235**, Part 1 & 2, 139 (1997).
[13] J. Ding, P. G. McCormick, and R. Street, J. Magn. Magn. Mater. **171**, 309 (1997).
[14] W. A. Kaczmarek, J. Magn. Magn. Mater. **157–158**, 264 (1996).
[15] C. Jocalekic, M. Zdujic, A. Radakovic, and M. Mitric, Mater. Lett. **24**, 365 (1995).
[16] R. F. Ziolo, E. P. Giannelis, B. A. Weinstein, M. P. O'Horo, B. N. Ganguly, V. Mehrotra, M. W. Russell, and D. R. Huffman, Science **257**, 219 (1992).
[17] B. H. Sohn, R. E. Cohen, and G. C. Papaefthymiou, J. Magn. Magn. Mater. **182**, 216 (1998).
[18] C. Castro, J. Ramos, A. Millan, J. G. Calbet, and F. Palacio, Chem. Mater. **12**, 3681 (2000).
[19] F. D. Monte, M. P. Morales, D. Levy, A. Fernandez, M. Ocana, A. Roig, E. Molins, K. O'Grady, and C. J. Serna, Langmuir **13**, 3627 (1997).
[20] F. Bentivegna *et al.*, J. Appl. Phys. **83**, 7776 (1998).
[21] V. Papaefthymiou, A. Kostikas, A. Simopoulos, D. Niarchos, S. Gangopadyay, G. C. Hadjupaayis, C. M. Sorensen, and K. J. Kablunde, J. Appl. Phys. **67**, 4487 (1990).
[22] M. I. Baraton, G. Busca, V. Lorenzelli, and B. J. Willey, J. Mater. Sci. Lett. **13**, 275 (1994).
[23] L. V. Gasparov, D. B. Tanner, D. B. Romero, H. Berger, G. Maritondo, and L. Forro, Phys. Rev. B **62**, 7939 (2000).
[24] M. H. Sousa, F. A. Tourinho, and J. C. Rubim, J. Raman Spectrosc. **31**, 185 (2000).
[25] P. R. Graves, C. Johnston, and J. J. Campaniello, Mater. Res. Bull. **23**, 1651 (1988).
[26] Y. Shi, J. Ding, Z. X. Shen, W. X. Sun, and L. Wang, Solid State Commun. **115**, 237 (2000).
[27] F. D. Monte, M. P. Morales, D. Levy, A. Fernandez, M. Ocana, A. Roig, E. Molins, K. Ogrady, and C. J. Serna, Langmuir **13**, 3627 (1997).
[28] J. M. Xue, Z. H. Zhou, and J. Wang, J. Am. Ceram. Soc. (in press).
[29] A. Regazzoni and E. Matijevic, Corrosion (Houston) **38**, 212 (1982).
[30] Z. H. Zhou, J. Xue, H. S. O. Chan, and J. Wang, J. Appl. Phys. **90**, 4169 (2001).
[31] A. C. Nunes and L. Yang, Surf. Sci. **399**, 225 (1998).
[32] A. E. Berkowitz, R. H. Kodama, S. A. Makhlouf, F. T. Parker, F. E. Spada, E. J. McNiff, Jr., and S. Foner, J. Magn. Magn. Mater. **196–197**, 591 (1999).
[33] J. A. Mydosh, *Spin Glasses: An Experimental Introduction* (Taylor & Francis, London, 1993).
[34] D. Bersani, P. P. Lottici, and A. Montenero, J. Raman Spectrosc. **30**, 355 (1999).
[35] J. Kreisel, G. Lucazeau, and H. Vincent, J. Solid State Chem. **137**, 127 (1998).
[36] D. L. Wood and E. M. Rabinovich, Appl. Spectrosc. **43**, 263 (1989).